Radiosensitizing effect of PSMC5, a 19S proteasome ATPase, in H460 lung cancer cells

Ji-Hye Yim [a, 1], Hong Shik Yun [a, b, 1], Su-Jae Lee [b], Jeong-Hwa Baek [a, c], Chang-Woo Lee [c], Ji-Young Song [a], Hong-Duck Um [a], Jong Kuk Park [a], Jae-Sung Kim [a], In-Chul Park [a], Sang-Gu Hwang [a, *]

[a] Division of Radiation Cancer Biology, Korea Institute of Radiological & Medical Sciences, Seoul 01812, Republic of Korea
[b] Department of Life Science, College of Natural Sciences, Hanyang University, Seoul 133-791, Republic of Korea
[c] Department of Molecular Cell Biology, Samsung Biomedical Research Institute, Sungkyunkwan University School of Medicine, Suwon 440-746, Republic of Korea

ARTICLE INFO

ABSTRACT

The function of PSMC5 (proteasome 26S subunit, ATPase 5) in tumors, particularly with respect to cancer radioresistance, is not known. Here, we identified PSMC5 as a novel radiosensitivity biomarker, demonstrating that radiosensitive H460 cells were converted to a radioresistance phenotype by PSMC5 depletion. Exposure of H460 cells to radiation induced a marked accumulation of cell death-promoting reactive oxygen species, but this effect was blocked in radiation-treated H460 PSMC5-knockdown cells through downregulation of the p53-p21 pathway. Interestingly, PSMC5 depletion in H460 cells enhanced both AKT activation and *MDM2* transcription, thereby promoting the degradation of p53 and p21 proteins. Furthermore, specific inhibition of AKT with triciribine or knockdown of MDM2 with small interfering RNA largely restored p21 expression in PSMC5-knockdown H460 cells. Our data suggest that PSMC5 facilitates the damaging effects of radiation in radiation-responsive H460 cancer cells and therefore may serve as a prognostic indicator for radiotherapy and molecular targeted therapy in lung cancer patients.

1. Introduction

Radiotherapy is commonly used to treat lung cancer, although it can also damage normal cells. However, intrinsic and acquired cellular radioresistance is a major impediment to improving the survival rate of non-small cell lung cancer (NSCLC) patients [1]. Despite several preclinical and clinical trials designed to improve the beneficial effects of radiotherapy, the mechanisms that promote radioresistance in NSCLC have not been fully investigated. The development and incorporation of molecular targeted therapeutics—the most prominent recent advance in the cancer research field [2]—illustrates the potential synergy of radiation combined with targeted therapy and underscores the need to overcome radioresistance problems in lung cancer, particularly in NSCLC patients.

The 26S proteasome is a multi-catalytic proteinase complex consisting of the 20S core particle and a set of 19S regulatory proteins [3]. Human PSMC5 (proteasome 26S subunit, ATPase 5), also known as SUG1, TRIP1 (thyroid hormone receptor-interacting protein 1) and TBP10 (Tat-binding protein homolog 10), among others, is a 19S regulatory component that can recognize ubiquitin-labeled proteins, converting them into a form suitable for degradation by the 20S complex. In addition to participating in proteasome function, PSMC5 is directly involved in regulating mammalian transcription through its association with transcriptionally active promotors and recruitment of coactivators. For example, this subunit plays a critical role in MHC class II transcription by regulating the activity of class II transactivator CIITA [4] and in p53-mediated p21 transcription by recruiting p53 to the p21 promoter region in response to ultraviolet radiation-induced DNA damage [5]. It has recently been reported that PSMC5 acts as a critical effector in osteoblast disease by causing cytodifferentiation

to osteoclasts [6] and in lung fibrotic pathology by modulating fibroblast trans-differentiation to a myofibroblast phenotype [7]. However, the association and function of PSMC5 in tumors, especially in terms of cellular mechanisms related to radiotherapy resistance, have not been explored.

In the present study, we report that PSMC5 knockdown in radiosensitive H460 NSCLC cells enhanced the ability of these cells to resist apoptosis in response to radiation. This acquisition of a radioresistance phenotype was attributable to diminished reactive oxygen species (ROS) generation through inhibition of p53-p21 signaling. The upstream signaling event in this action of PSMC5 depletion was induction of both AKT activation and MDM2 expression, which promoted p53-p21 protein degradation. Therefore, we propose PSMC5 as a novel potential biomarker for molecular targeted therapeutic strategies in radioresistant lung cancer patients.

2. Materials and methods

2.1. Cell culture and treatment

Human H460 cells were purchased from ATCC (Manassas, VA, USA). A radioresistant derivative (RR-H460) was established from H460 cells as described previously [8]. Cells were cultured in RPMI-1640 medium containing 10% fetal bovine serum. Cells were irradiated using a ^{137}Cs-ray source (Atomic Energy of Canada, Ltd., Mississauga, Canada) at a dose rate of 3.81 Gy/min and treated with 10 μM triciribine (Calbiochem, San Diego, CA, USA) to inhibit AKT activity.

2.2. Gel electrophoresis and mass spectrometry analysis

Parental H460 and RR-H460 cell lines were solubilized in 200 μl of polyacrylamide gel electrophoresis buffer (9 M urea, 40 mM Tris, 4% CHAPS, pH 8.5), disrupted with a probe sonicator (Branson Ultrasonic Corporation, Danbury, USA), and centrifuged at 12000 rpm for 15 min. Cell lysates (150 μg) were resolved by two-dimensional polyacrylamide gel electrophoresis (2-D PAGE) as described previously [8]. All protein spots in gels were visualized using the silver staining method and then digested with 10 ng/mL trypsin (Promega, Madison, WI, USA). Dried tryptic peptides were analyzed by mass spectrometry, and proteins were identified by peptide mass fingerprinting as described previously [8].

2.3. Oncomine data mining

Oncomine (Life Technologies, Ann Arbor, MI, USA) was used for data analysis and visualization as described previously [9]. PSMC5 expression was compared in lung cancer and normal lung tissue extracts.

2.4. Immunohistochemistry

Human tissue microarrays were purchased from SuperBioChips (Cat Number: CC5; Seoul, Korea), and immunohistochemistry was performed using an anti-PSMC5 mouse monoclonal antibody (1:250 dilution; Santa Cruz Biotechnology Inc., Santa Cruz, CA, USA) as described previously [10]. Immunostaining was performed using the avidin-biotin-peroxidase method according to the manufacturer's instructions (Invitrogen, Carlsbad, CA, USA). Staining intensity was scored as follows: 0 (no visible staining), 1 + (faint staining), 2 + (moderate staining), and 3 + (strong staining).

2.5. Quantitative reverse transcription-polymerase chain reaction (qRT-PCR)

Transcripts were quantified by qRT-PCR as described previously [8] using the following primer pairs: PSMC5 (150-bp product), 5′-AGA ATG GTG AGG GAG CTG TT-3′ (sense) and 5′-GTT GAG CAA CTC CAG CAT CG-3′ (antisense); p53 (361-bp product), 5′-GTG GTG CCC TAT GAG CCG CC-3′ (sense) and 5′-GCT CAC GCC CAC GGA TCT GA-3′ (antisense); p21 (74-bp product), 5′-GGC AGA CCA GCA TGA CAG ATT-3′ (sense) and 5′-GCG GAT TAG GGC TTC CTC T-3′ (antisense); MDM2 (259-bp), 5′-AAG ACT ATT CTC AGC CAT CA-3′ (sense) and 5′-CAT ACT GGG CAG GGC TTA-3′ (antisense); and glyceraldehyde-3-phosphate dehydrogenase (GAPDH; 305-bp product), 5′-CAT CTC TGC CCC CTC TGC TGA-3′ (sense) and 5′-GGA TGA CCT TGC CCA CAG CCT-3′ (antisense).

2.6. Cell death assay

Cell death was quantified as described previously [8]. Apoptotic cell death was also determined by Western blot analysis of cleaved poly (ADP-ribose) polymerase (PARP) and activated caspase-3.

2.7. Colony-forming assay

Cell survival was determined by clonogenic survival assays, as described previously [8]. Briefly, cells were seeded into triplicate 60-mm tissue culture dishes at densities of 1.2, 6.0, and 12.0 × 10³ cells/dish and exposed to 0, 4, and 6 Gy radiation, respectively. Cells were exposed once to the indicated doses of radiation. After 14 d, colonies arising from surviving cells were stained with trypan blue solution and counted using a colony counter (Imaging Products, Chantilly, VA, USA).

2.8. ROS assay

Cells were incubated with 10 nM 2′,7′-dichlorofluorescein diacetate (DCF-DA; Molecular Probes, Inc., Eugene, OR, USA) for 20 min to detect ROS, as described previously [8].

2.9. Knockdown of proteins by small interfering RNA (siRNA)

The following human-specific siRNAs, synthesized as described by the manufacturer (Genolution, Seoul, Korea), were used: siPSMC5 #1, 5′-CCA AGA ACA UCA AGG UUA UUU-3′ (sense) and 5′-AUA ACC UUG AUG UUC UUG GUU-3′ (antisense); siPSMC5 #2, 5′-GUG UGU AUC UCU CCA AUA AUU-3′ (sense) and 5′-UUA UUG GAG AGA UAC ACA CUU-3′ (antisense); siPSMC5 #3, 5′-GUU AUC AUG GCU ACU AAU AUU-3′ (sense) and 5′-UAU UAG UAG CCA UGA UAA CUU-3′ (antisense); and siMDM2, 5′-AAU GCC UCA AUU CAC AUA GAU UU-3′ (sense) and 5′-AUC UAU GUG AAU UGA GGC AUU UU-3′ (antisense). A scrambled siRNA that showed no significant homology to known gene sequences was used as a negative control. For experiments, cells were transiently transfected with 20 nM siPSMC5 #3 or siMDM2 in medium as described previously [8].

2.10. Immunofluorescence confocal microscopy

Immunofluorescence staining for p21 (BD Pharmingen, San Jose, CA, USA), pAKT (Ser473; Cell Signaling Technology Inc., Beverly, MA, USA), and MDM2 (Santa Cruz Biotechnology Inc.) was performed as described previously [8]. Cell nuclei were identified by staining with 4.6-diamidino-2-phenylindole (DAPI).

2.11. Western blot analysis

Western blot analyses were done as described previously [8] using primary antibodies against cleaved-PARP (Asp214), cleaved caspase-3, phospho-AKT (Ser473), AKT, and phopho-p53 (Ser15) (Cell signaling Technology Inc.); p53, PSMC5 and MDM2 (Santa Cruz Biotechnology Inc.); and p21 (BD Pharmingen). β-actin (Sigma-Aldrich, St. Louis, MO, USA) was used as a loading control.

2.12. Statistical analysis

Cell culture experiments were repeated at least three times. All data are expressed as means ± standard deviation. Statistical evaluations were conducted using a one-way analysis of variance (ANOVA). A P-value < 0.05 was considered significant.

3. Results

3.1. Identification of PSMC5 as a radiosensitivity biomarker in H460 cells

We established RR-H460 cells from radiosensitive parental H460 cells by exposing them to 2 Gy radiation twice a week for 15 wk (data not shown) and analyzed the protein expression profiles between these two cell lines using 2-D PAGE analysis. Among the spots showing differential expression was that for PSMC5, which was downregulated more than 2-fold in RR-H460 cells (Fig. 1A), suggesting that it might be involved in radiosensitivity. This

decrease is shown more clearly in magnified images of PSMC5 spots in gel images of parental H460 and RR-H460 cells, and was confirmed by Western blot analysis (Fig. 1B). The identity of this spot as PSMC5 was determined by MALDI-TOF mass spectrometry analysis, with excellent peptide coverage and a significant MASCOT score (Fig. 1C).

We also examined the correlation between PSMC5 expression and lung cancer severity using the human genetic dataset analysis tool, Oncomine. PSMC5 mRNA levels were significantly lower in lung carcinoid tumors (Fig. 1D, left) and lung adenocarcinoma tumors (Fig. 1D, right) compared with normal lung tissue, suggesting that PSMC5 functions as a tumor-suppressor. Consistent with Oncomine data, *in vivo* evidence from tissue microarrays containing lung cancers and their normal tissue counterparts showed that PSMC5 expression was downregulated in lung cancer tissue compared with their normal tissue counterparts (Fig. 1E). These results suggest that PSMC5 knockdown could play a pivotal role in acquisition of the radioresistance phenotype and tumorigenesis of H460 cells.

3.2. PSMC5 knockdown inhibits radiation-induced apoptosis of H460 cells

To examine whether PSMC5 plays a pivotal role in the regulation of radiation-induced cell death, we transfected H460 cells with siRNA to knock down endogenous PSMC5. As shown in Fig. 2A, all three siRNAs markedly decreased PSMC5 protein and transcript levels: qRT-PCR results showed that the most effective was siRNA
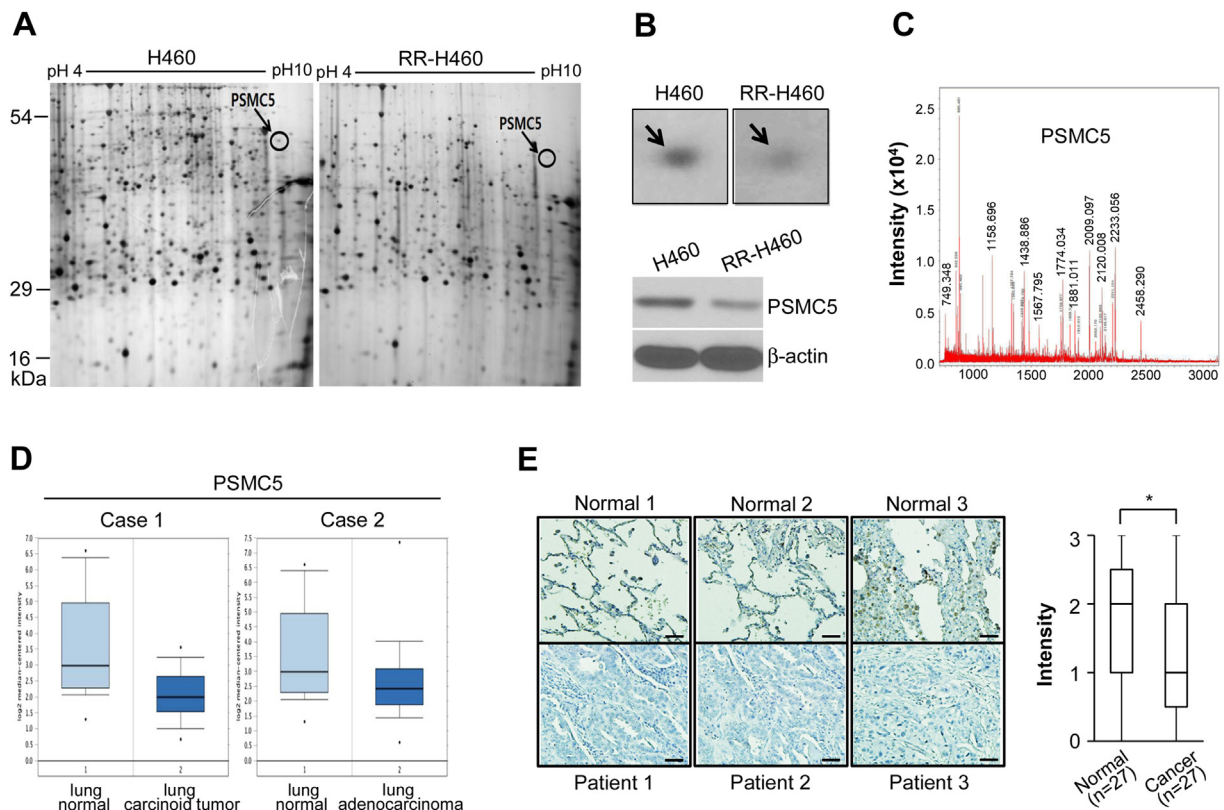

Fig. 1. Identification of PSMC5 as a radiosensitivity biomarker in H460 cancer cells. (A) 2D-gel analysis of differentially expressed proteins between parental H460 and RR-H460 cells. PSMC5 spots are marked by black arrows in each panel. (B) Magnified view (top) and expression level (bottom) of PSMC5 shown in A. Expression level was determined by Western blotting. (C) MALDI-TOF/MS analysis of PSMC5. (D) Available datasets in the Oncomine database were queried for PSMC5 expression with respect to cancer versus normal tissue (Case 1: threshold P-value = 9.81×10^{-4}, fold change ≥ 2; Case 2: threshold P-value = 0.019, fold change ≤ 2). (E) Representative microscopic images of sections of lung cancer and their normal tissue counterparts stained with anti-PSMC5 antibody (scale bar: 1 mm). Staining intensity was scored as described in Materials and Methods; data are presented as box-and-whisker plots (*P < 0.05 compared with staining intensity of normal tissues).
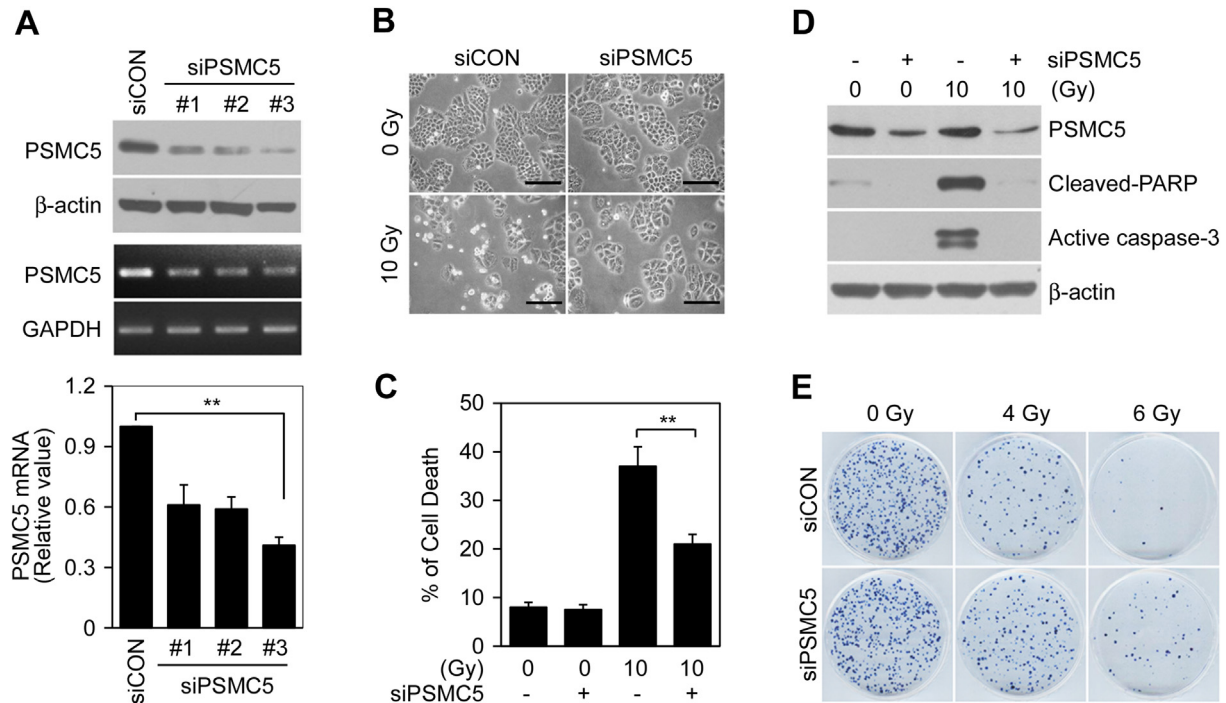
Fig. 2. PSMC5 knockdown inhibits radiation-induced apoptosis of H460 cells. (A) H460 cells were transfected with 20 nM control siRNA (siCON) or three PSMC5 siRNAs (siPSMC5) for 48 h. Protein and transcript levels of PSMC5 were determined by Western blotting (top) and conventional PCR (middle; loading control: GAPDH), respectively. qRT-PCR data (bottom) are expressed as means ± SD (**$P < 0.005$ compared with untransfected control). (B–D) H460 cells were transfected with 20 nM siCON or PSMC5 siRNA #3 for 5 h and then treated without or with 10 Gy radiation for an additional 48 h. Morphological changes were observed by light microscopy. Scale bars: 0.1 mm (*B*). Cell death was determined by FACS analysis; data are expressed as means ± SD (**$P < 0.005$ compared with cells treated with radiation alone) (*C*). Protein levels of PSMC5 and two apoptosis markers were determined by Western blotting (*D*). (E) H460 cells were transfected with 20 nM siCON or PSMC5 siRNA #3 for 24 h and then treated with single doses of radiation (0–6 Gy). Representative images of colony formation at 14 d after radiation treatment, visualized by trypan blue staining, are shown.

#3, which reduced mRNA levels by approximately 60% compared to control siRNA. An assessment of cell morphology by light microscopy revealed that treatment of H460 cells with 10 Gy radiation very effectively induced cell death, an effect that was markedly inhibited by PSMC5 knockdown (Fig. 2B). The death rate in H460 cells treated with radiation alone was approximately 37% compared to approximately 18% in PSMC5-transfected, radiation-treated H460 cells, as determined by fluorescence-activated cell sorting (FACS) analysis (Fig. 2C). Consistent with FACS and microscopy results, the levels of cleaved-PARP and active caspase-3, two standard apoptosis markers, were markedly increased in radiation-treated H460 cells; these effects too were completely inhibited by PSMC5 depletion (Fig. 2D). Clonogenic survival assays showed that PSMC5-depleted H460 cells displayed a more radioresistant phenotype than control cells in response to a single dose of radiation ranging from 0 to 6 Gy (Fig. 2E). Therefore, our results suggest that PSMC5 acts as a radiosensitive molecular target that mediates radiation-induced cytotoxicity of H460 cells.

3.3. PSMC5 knockdown inhibits ROS generation and p21 protein expression induced by radiation treatment in H460 cells

To determine whether PSMC5 is associated with the generation of ROS, an important effector of radiation-induced apoptosis, we transfected H460 cells with siRNA to knock down endogenous PSMC5 and measured ROS levels by monitoring fluorescence of the ROS indicator, DCF-DA. Depletion of PSMC5 had little effect on ROS levels in H460 cells in the absence of radiation exposure, but significantly suppressed the marked increase in ROS levels induced by 6 Gy radiation treatment, as determined by cell staining (Fig. 3A). FACS analysis showed that ROS levels were increased by approximately 2.6-fold in radiation-treated H460 cells and were

reduced by approximately 1.4-fold in PSMC5-knockdown H460 cells compared to nonirradiated cells (Fig. 3B), indicating that PSMC5 positively regulates radiation-induced ROS generation. We further tested whether ROS production is associated with levels of the ROS-inducing apoptosis regulators, p53 and p21. Interestingly, we found that silencing of PSMC5 alone markedly decreased p53 and p21 protein levels in H460 cells (Fig. 3C, left) without changing their transcript levels (Fig. 3C, right), suggesting regulation of protein stability. As expected, exposure of H460 cells to radiation induced a time-dependent activation (phosphorylation) of p53 and induction of p53 and p21 protein levels without altering PSMC5 protein level (Fig. 3D). However, radiation-induced p53 and p21 protein levels, which peaked 6 and 12 h after radiation treatment, respectively (Fig. 3E), were markedly reduced by PSMC5 depletion. p21 transcript levels were did not changed by PSMC5 knockdown, as determined by conventional PCR (Fig. 3F, top) and qRT-PCR (Fig. 3C, bottom); radiation-induced increases in p53 transcript levels were similarly unaffected by PSMC5 knockdown (data not shown). We next tested p21 protein localization, because it has been shown that this is important for the control of cell survival. As shown in Fig. 3G, p21 protein was mainly localized in the nucleus of control H460 cells and was not redistributed by stimulation with radiation and/or PSMC5 knockdown, although expression levels were changed, consistent with the results of Western blot analyses. Taken together, our data suggest that PSMC5 signaling is essential for promoting cell death in radiation-treated H460 cells.

3.4. Downregulation of p21 protein in H460 cells by PSMC5 depletion is attributable to stabilization of AKT and MDM2

Because MDM2 activation by phosphoinositide 3-kinase (PI3K)/ AKT signaling acts as a negative regulator of p21 degradation in a
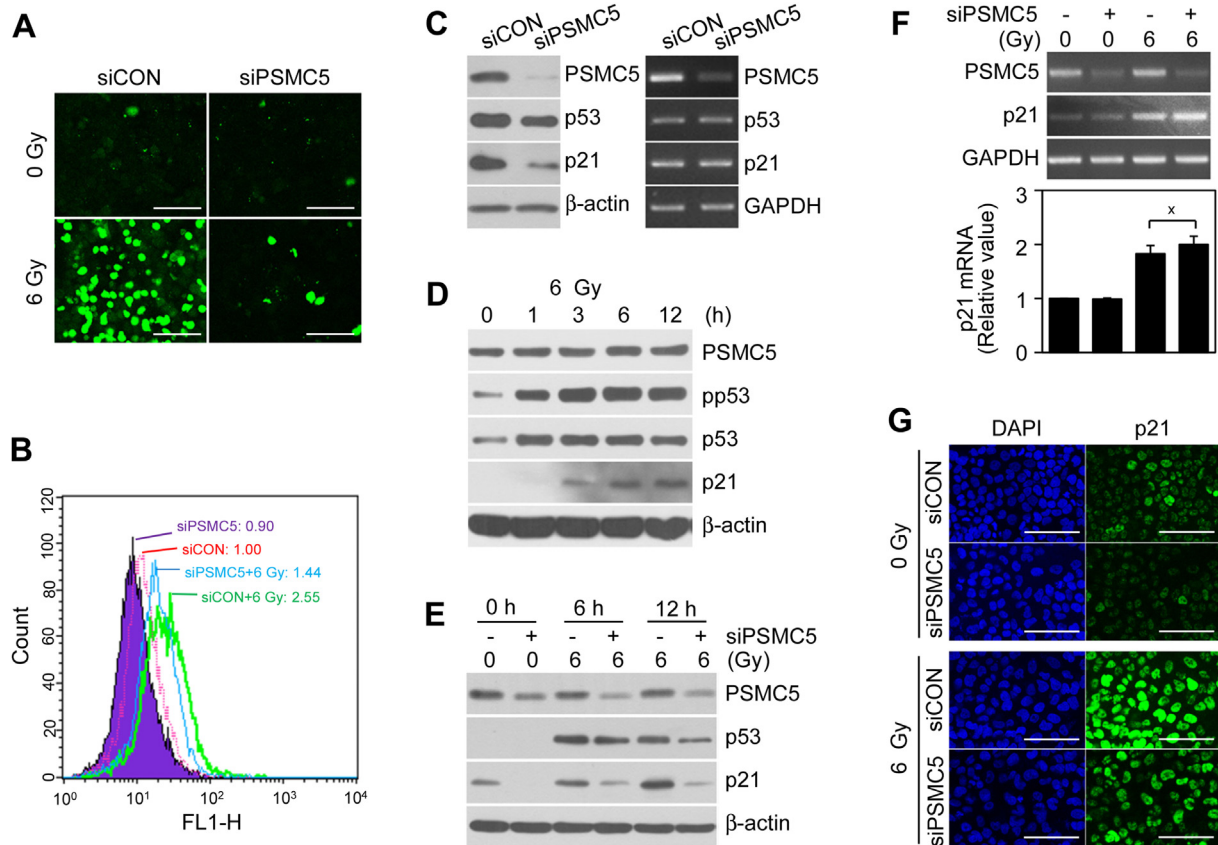
Fig. 3. PSMC5 knockdown inhibits ROS generation and radiation-induced expression of p53 and p21 protein in H460 cells. (A and B) H460 cells were transfected with 20 nM control siRNA (siCON) or PSMC5 siRNA #3 (siPSMC5) for 24 h and then treated without or with 6 Gy radiation for an additional 24 h. Intracellular ROS levels were determined by fluorescence confocal microscopy (A; scale bar: 1 mm) and analyzed by FACS using 10 μM DCF-DA (B). (C) H460 cells were transfected with 20 nM siCON or PSMC5 siRNA #3 for 48 h. Protein (left) and transcript (right) levels of PSMC5, p53, and p21 were determined by Western blotting and conventional PCR (loading control: GAPDH), respectively. (D) H460 cells were treated with 6 Gy radiation for the indicated times. Protein levels of PSMC5, p53 and p21, and phosphorylation levels of p53 (pp53) were determined by Western blotting. (E) H460 cells were transfected as in A and then treated without or with 6 Gy radiation for an additional 6 or 12 h. Protein levels of PSMC5, p53, and p21 were determined by Western blotting. (F and G) H460 cells were transfected as in A and then treated without or with 6 Gy radiation for an additional 12 h. The presence of p21 transcripts was monitored by conventional PCR (F, top; loading control: GAPDH), and p21 mRNA levels were determined by qRT-PCR (F, bottom). qRT-PCR data are expressed as means ± SD (^{x} denotes no significance compared with cells treated with radiation alone). p21 localization was visualized by confocal microscopy; representative images are shown (G). Scale bar: 1 mm.

p53-independent manner [11,12], we examined whether the AKT-MDM2 pathway is involved in PSMC5-depletion-mediated downregulation of p21 protein. Notably, we found that PSMC5 knockdown led to induction of AKT phosphorylation at Ser473 in H460 cells without changing basal AKT expression levels, consistent with the observed upregulation of MDM2 protein (Fig. 4A, left) and mRNA (Fig. 4A, right) levels, the latter of which were increased by approximately 1.8-fold in PSMC5-knockdown H460 cells compared to control cells. MDM2 protein was predominantly localized to the nucleus in control H460 cells and its distribution was unaffected by PSMC5 depletion (Fig. 4B, top). Interestingly, phosphorylated AKT was located in both cytosol and nucleus in control H460 cells, but its nuclear localization was increased in PSMC5-knockdown H460 cells (Fig. 4B, bottom), presumably reflecting the association of AKT activation with MDM2 transcript levels. Furthermore, exposure of H460 cells to radiation reduced AKT phosphorylation and MDM2 protein levels compared with control cells, affects that were markedly attenuated by PSMC5 depletion (Fig. 4C). Finally, we confirmed the association of PSMC5-mediated p21 regulation with the AKT-MDM2 pathway using an AKT or MDM2 loss-of-function approach. Notably, the level of p21 protein, which was significantly reduced in association with a striking increase in activating AKT phosphorylation in radiation-treated, PSMC5-knockdown H460 cells, was completely recovered by treatment with

triciribine, a specific inhibitor of AKT (Fig. 4D), indicating that p21 protein is a downstream target of the AKT pathway. The reduction of p21 levels in PSMC5-knockdown H460 cells was also restored by silencing of MDM2, consistent with the fact that MDM2 is an upstream regulator of p21 protein degradation (Fig. 4E). Taken together, our data indicate that acquisition of a radioresistant phenotype in PSMC5-depleted H460 cells is attributable to p21 degradation through AKT-dependent MDM2 stabilization.

4. Discussion

We detected approximately 2000 differentially expressed proteins between radiosensitive parental H460 cells and their radioresistant derivative. A total of 23 protein spots were downregulated in radioresistant H460 cells, eight of which were altered by more than 2-fold, including PSMC5, a regulatory ATPase subunit of the 26S proteasome. Because the 26S proteasome system is involved in the ATP-dependent degradation of ubiquitinated proteins, PSMC5 may play a crucial role in maintaining cellular proteome homeostasis in a variety of situations [3]. This subunit is now known to play roles in controlling transcriptional regulation [4,5], but PSMC5 modulation as a contributor to tumor resistance and progression has not been investigated. The present study provides the first evidence for the novel function of PSMC5 in the susceptibility of
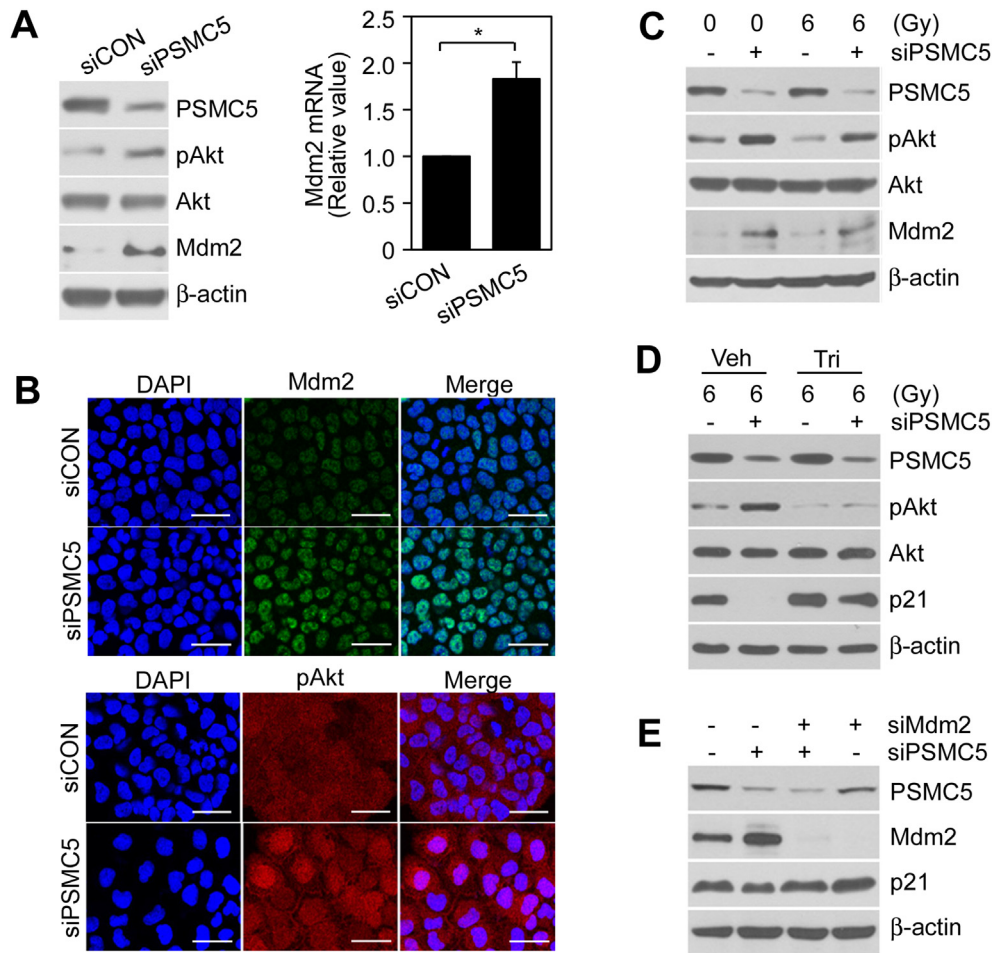
Fig. 4. PSMC5 knockdown induces degradation of p21 protein through activation of AKT-MDM2 in H460 cells. (A and B) H460 cells were transfected with 20 nM siCON (siCON) or PSMC5 siRNA #3 (siPSMC5) for 48 h. Protein levels of PSMC5, AKT and MDM2, and phosphorylation levels of AKT (pAKT) were determined by Western blotting (A, left). MDM2 transcript levels were determined by qRT-PCR (A, right); data are expressed as means ± SD (*$P < 0.05$ compared with untransfected control). MDM2 and phosphorylated-AKT localization was visualized by confocal microscopy; representative images are shown (B; scale bar: 0.5 mm). (C) H460 cells were transfected with 20 nM siCON or PSMC5 siRNA #3 for 24 h and then treated without or with 6 Gy radiation for an additional 24 h. Protein levels of PSMC5, AKT and MDM2, and phosphorylation levels of AKT were detected by Western blotting. (D) H460 cells were transfected as in C and then treated without or with 6 Gy radiation in the absence (Veh) or presence (Tri) of 10 μM triciribine for an additional 24 h. Protein levels of PSMC5, AKT and p21, and phosphorylation levels of AKT were detected by Western blotting. (E) H460 cells were transfected with 20 nM siCON or PSMC5 siRNA #3 and/or 20 nM MDM2 siRNA, as indicated, for 48 h. Protein levels of PSMC5, MDM2, and p21 were determined by Western blotting.

tumors to the injurious actions of radiation.

Erina et al. provided evidence that constitutively reduced 26S proteasome activity increases self-renewal capacity in glioma and breast cancer cells, and is thus associated with clinical resistance to radiation therapy [13]. Intrinsically low 26S proteasome activity, which is responsible for the resistance to proteasome inhibitors and radiation treatment, has been shown to contribute to the failure of clinical trials in advanced prostate cancer [14]. Consistent with these observations, we found that loss of PSMC5 function inhibits radiation-induced cell death in H460 cancer cells (Fig. 2). Proteasome activity plays a fundamental role in many cellular processes, including cell-cycle regulation, gene expression and cell differentiation, and has therefore become an important target for anticancer therapy. Proteasome inhibitors have been suggested as promising new agents against solid tumors, but initial results from clinical trials have shown little antitumor activity—a failure attributable to cancer cells with a low-proteasome-activity phenotype [14]. In keeping with this, our findings suggest the additional possibility that PSMC5 plays an important role as a radiosensitizing factor in lung cancer cells; thus, its low activity is responsible for the radioresistance of RR-H460 NSCLC cells.

Because it is unknown why PSMC5 depletion promotes resistance to radiation in H460 cells, it will be important to investigate how PSMC5 knockdown contributes to radiation-induced changes in cell functions, such as proliferation and apoptosis. Our demonstration of PSMC5 knockdown-dependent AKT phosphorylation is in accord with a previous report showing an association of AKT activation with the radioresistance phenotypes of different cancers, including colon, prostate, and brain cancer [15]. In addition, the MDM2 oncoprotein is overexpressed in many human malignancies and its nuclear localization is dependent on its interaction with activated AKT [11,15]. This cascade stimulates formation of a complex of MDM2 with p21 and p53 that promotes ubiquitin-independent or -dependent degradation of p21 and p53 [12,16]. In this study, AKT, activated by PSMC5 depletion, was predominantly translocated into the nucleus, enhancing the nuclear accumulation of MDM2 protein. Furthermore, inhibition of AKT signaling or MDM2 expression strongly restored p21 protein levels that were decreased by PSMC5 knockdown in H460 cells (Fig. 4), indicating that the AKT-MDM2 pathway is involved in the radioresistance phenotype as a negative regulator of p21. Intracellular ROS are important mediators of apoptosis and their regulation was

dependent on the levels of p21 expression (Fig. 3), suggesting that p21-mediated ROS production could also participate in cell fate decisions.

In conclusion, PSMC5 depletion modulated the radiosensitivity of H460 NSCLC cells by activating AKT-MDM2 signaling and, in turn, triggering a decrease in p53 and p21 activity, thereby contributing to acquisition of radioresistance. Therefore, PSMC5 status could serve as a prognostic indicator for radiotherapy, and restoring PSMC5 activity might represent an alternative strategy for treating cancer when serious resistance to radiotherapy is present.

Conflict of interest

The authors have declared no conflict of interest.

Acknowledgments

References

[1] Z.J. Yin, F.G. Jin, T.G. Liu, E.Q. Fu, Y.H. Xie, R.L. Sun, Overexpression of STAT3 potentiates growth, survival, and radioresistance of Non-Small-Cell Lung Cancer (NSCLC) cells, J. Surg. Res. 171 (2011) 675—683.

[2] Z.S. Morris, P.M. Harari, Interaction of radiation therapy with molecular targeted agents, J. Clin. Oncol. 32 (2014) 2886—2893.

[3] M. Rechsteiner, L. Hoffman, W. Dubiel, The multicatalytic and 26 S proteases, J. Biol. Chem. 268 (1993) 6065—6068.

[4] K.P. Bhat, J.D. Turner, S.E. Myers, A.D. Cape, J.P. Ting, S.F. Greer, The 19S proteasome ATPase Sug1 plays a critical role in regulating MHC class II transcription, Mol. Immunol. 45 (2008) 2214—2224.

[5] Q. Zhu, G. Wani, J. Yao, S. Patnaik, Q.E. Wang, M.A. El-Mahdy, M. Praetorius-Ibba, A.A. Wani, The ubiquitin-proteasome system regulates p53-mediated transcription at p21waf1 promoter, Oncogene 26 (2007) 4199—4208.

[6] D. Metz-Estrella, J.H. Jonason, T.J. Sheu, R.M. Mroczek-Johnston, J.E. Puzas, TRIP-1: a regulator of osteoblast function, J. Bone Miner. Res. 27 (2012) 1576—1584.

[7] M.F. Nyp, A. Navarro, M.H. Rezaiekhaligh, R.E. Perez, S.M. Mabry, I.I. Ekekezie, TRIP-1 Via AKT modulation drives lung fibroblast/myofibroblast trans-differentiation, Respir. Res. 15 (2014), 19—9921-15-19.

[8] J.S. Kim, J.W. Chang, H.S. Yun, K.M. Yang, E.H. Hong, D.H. Kim, H.D. Um, K.H. Lee, S.J. Lee, S.G. Hwang, Chloride intracellular channel 1 identified using proteomic analysis plays an important role in the radiosensitivity of HEp-2 cells via reactive oxygen species production, Proteomics 10 (2010) 2589—2604.

[9] H.S. Yun, J.H. Baek, J.H. Yim, S.J. Lee, C.W. Lee, J.Y. Song, H.D. Um, J.K. Park, I.C. Park, S.G. Hwang, Knockdown of hepatoma-derived growth factor-related protein-3 induces apoptosis of H1299 cells via ROS-dependent and p53-independent NF-kappaB activation, Biochem. Biophys. Res. Commun. 449 (2014) 471—476.

[10] J.S. Kim, E.J. Kim, J.S. Oh, I.C. Park, S.G. Hwang, CIP2A modulates cell-cycle progression in human cancer cells by regulating the stability and activity of Plk1, Cancer Res. 73 (2013) 6667—6678.

[11] L.D. Mayo, D.B. Donner, A phosphatidylinositol 3-kinase/Akt pathway promotes translocation of Mdm2 from the cytoplasm to the nucleus, Proc. Natl. Acad. Sci. U.S.A. 98 (2001) 11598—11603.

[12] Z. Zhang, H. Wang, M. Li, S. Agrawal, X. Chen, R. Zhang, MDM2 is a negative regulator of p21WAF1/CIP1, independent of p53, J. Biol. Chem. 279 (2004) 16000—16006.

[13] E. Vlashi, K. Kim, C. Lagadec, L.D. Donna, J.T. McDonald, M. Eghbali, J.W. Sayre, E. Stefani, W. McBride, F. Pajonk, In Vivo imaging, tracking, and targeting of cancer stem cells, J. Natl. Cancer Inst. 101 (2009) 350—359.

[14] L. Della Donna, C. Lagadec, F. Pajonk, Radioresistance of prostate cancer cells with low proteasome activity, Prostate 72 (2012) 868—874.

[15] S. Tanno, N. Yanagawa, A. Habiro, K. Koizumi, Y. Nakano, M. Osanai, Y. Mizukami, T. Okumura, J.R. Testa, Y. Kohgo, Serine/threonine kinase AKT is frequently activated in human bile duct cancer and is associated with increased radioresistance, Cancer Res. 64 (2004) 3486—3490.

[16] B.P. Zhou, Y. Liao, W. Xia, Y. Zou, B. Spohn, M.C. Hung, HER-2/neu induces p53 ubiquitination via Akt-mediated MDM2 phosphorylation, Nat. Cell Biol. 3 (2001) 973—982.